New Method for Testing Composites at Very High Strain Rates

A method was developed for testing and characterizing unidirectional and angle-ply composite laminates at strain rates in the 100 to 500 s^{-1} regime

by I.M. Daniel, R.H. LaBedz and T. Liber

ABSTRACT—A method was developed for testing and characterizing composite materials at strain rates in the 100 to 500 s^{-1} regime. The method utilizes a thin ring specimen, 10.16 cm (4 in.) in diameter, 2.54 cm (1 in.) wide and 6-8 plies thick. This specimen is loaded by an internal pressure pulse applied explosively through a liquid. Pressure is measured by means of a calibrated steel ring instrumented with strain gages. Strains in the composite specimen are measured with strain gages. Strains in the calibration and specimen rings are recorded with a digital processing oscilloscope. The equation of motion is solved numerically and the data processed by the mini-computer attached to the oscilloscope. Results are obtained, and plotted by an X-Y plotter in the form of a dynamic stress–strain curve. Unidirectional 0-deg, 90-deg and 10-deg off-axis graphite/epoxy rings were tested at strain rates up to 690 s^{-1}. Times to failure ranged between 30 and 60 μs. The 0-deg properties which are governed by the fibers do not vary much from the static ones with only small increases in modulus. The 90-deg properties show much higher than static modulus and strength. The dynamic in-plane shear properties, obtained from the 10-deg off-axis specimens, are noticeably higher than static ones. In all cases the dynamic ultimate strains do not vary much from the static values.

Introduction

The application of composites to dynamically loaded components and structures requires knowledge and understanding of the dynamic loading, induced-wave-propagation phenomena and the response of the material to the high strain rates produced. For example, composite jet-engine blades are exposed to the hazards of foreign object damage, such as bird impact on rotating blades. Such impacts occur at velocities up to 305 ms^{-1} (1000 ft/s) and can cause extensive damage to the composite blade. Similarly, in applications to protective armor or other components, composites are subjected to high-velocity impacts. These impact loadings are of short duration, of the order of 100 μs, and produce stress (strain) wave pulses with strain rates up to a few hundred (m/m) per second. Reliable design of composite components for impact resistance requires characterization of the composite material at high strain rates. Most composite materials have been amply characterized under quasi-static conditions. Little work on composite properties at high rates of loading has been reported.

Early attempts to measure dynamic properties in composites were limited to determination of elastic and viscoelastic constants by ultrasonic velocity measurements and vibration testing.[1-3] Attempts to characterize composites at high strain rates were made by Rotem and Lifshitz[4,5] and Armenakas and Sciammarella,[6] and the authors.[7,8] Most of this work deals with glass/epoxy composites at rates less than 100 s^{-1}. The type of specimen used in these cases was a coupon loaded through grips by means of a falling weight or ram of an electrohydraulic system. The rate at which such specimens are tested is limited by the transit time of the stress wave through the length of the specimen. Compressive properties of composites (steel-wire reinforced epoxy) were studied by Sierakowski *et al.* at strain rates up to 1000 s^{-1} using a split Hopkinson bar.[9] However, this test produces a multi-axial state of stress in the short cylindrical specimens used.

A variety of testing techniques and procedures have been developed for testing materials at high rates of loading. Different methods are suited for different ranges of strain rate. The low-strain-rate region is associated with creep. Standard hydraulic or screw machines are used for quasi-static loading of coupons at a constant strain rate. In the medium strain-rate region for strain rates up to approximately 50 s^{-1}, fast-acting hydraulic or pneumatic machines are used. Inertia forces begin to become important and possible mechanical resonances must be taken into account. In the medium-regime wave-propagation effects are neglected and uniform stresses and strains are assumed in the test specimen. Load is normally measured with a load cell connected in series with the specimen.

Higher strain rates, primarily in compression, can be obtained with mechanical impact from a fast moving mass or by explosively generated pulses. In the highest strain-rate regime, wave-propagation effects become very dominant and must be accounted for. This fact leads to many difficulties and causes a great deal of uncertainty on the interpretation of results. For this reason, the scant data available in this high-strain-rate region are of doubtful validity.

The wave-propagation effects are virtually eliminated by utilizing a thin ring specimen loaded with a dynamic internal-pressure pulse, because the transit time of the wave across the thickness of the specimen is very short. This paper describes the development and application of this method for testing and characterization of composite

I.M. Daniel (SESA Member) and R.H. LaBedz are Science Advisor and Technical Assistant, respectively, Materials Technology Division, IIT Research Institute, Chicago, IL 60616. T. Liber is Staff Specialist, Travenol Laboratories, Round Lake, IL 60073.

Paper was presented at Fourth SESA International Congress on Experimental Mechanics held in Boston, MA on May 25-30, 1980.

Revised version received: August 3, 1980.

materials at high strain rates. Longitudinal, transverse and in-plane shear properties, including modulus, Poisson's ratio, strength, and ultimate strain, were determined.

Experimental Procedure

The material used in this development was SP288/AS graphite/epoxy (3M Company). It was used in the form of 6-ply and 8-ply unidirectional laminates.

A thin ring specimen 10.16 cm (4 in.) in diameter, 2.54 cm (1 in.) wide and 6-8 plies thick was used. Graphite/epoxy rings with the fibers at 0-, 90- and 10-deg with the circumferential direction were used. The ring specimens used were cut from longer composite tubes, which can be fabricated with any desired ply orientation and stacking sequence. The fabrication procedure for such tubes was described in detail by the authors recently.[10] The tooling consists mainly of a perforated hollow stainless-steel mandrel covered with a silicon-rubber bladder and two outer halves forming the cylindrical mold cavity. Vent, separator, bleeder and composite-prepreg plies are wrapped in sequence over the bladder. The mold is assembled and sealed around the layup and the laminate is cured in an oven with internal pressure acting through the perforated mandrel and vacuum drawn. After fabrication, tube quality is assessed in three different ways. The tube is inspected ultrasonically, its laminate thickness is measured at various points, and the hoop strength is measured directly by cutting rings from the ends and testing them statically under internal pressure. A special tooling fixture is used for cutting ring specimens from the tubes. Elastic and ultimate properties obtained from instrumented rings indicate that composite tubes can be fabricated with the same properties as flat laminates.

Ring specimens were loaded by an internal pressure pulse applied explosively through a liquid in a specially designed fixture. This fixture consists of two thick cylinders and two disks assembled together with the ring specimen between them (Figs. 1 and 2). The reservoir is filled with a mixture of water and water-soluble oil. The pressure pulse in the chamber was produced by detonating an explosive charge in the liquid reservoir. In the case of the $[90_8]$ specimens 260 mg (4 grains) of pistol powder was used. In the case of the $[0_6]$ and $[10_8]$ specimens 100 mg and 330 mg PETN detonators, each containing 110-mg lead-azide priming charge, were used. The resulting strain rates depend on the amount and rate of burning of the explosive and the specimen stiffness. The explosive sizes were varied with the various specimens to obtain strain rates in the same range.

The dynamic internal pressure originally was measured with a piezoelectric transducer mounted on the side of the cylinder. Because of the large noise of the pressure signals obtained, this transducer was replaced by a steel calibration ring placed next to the composite ring specimen. This ring had an internal diameter of 9.957 cm (3.920 in.), a width of 1.27 cm (0.5 in.) and a thickness of 1.44 mm (0.056 in.). It was made of Vascomax steel which is an 18-percent-nickel maraging steel with a 2415 MPa (350 ksi) yield point and 193 GPa (28×10^6 psi) modulus. The ring was calibrated statically under internal pressure. It was also shown that Vascomax steel does not exhibit any strain-rate effects, by conducting wave-propagation tests and measuring the propagation velocity.

Strains in the composite and steel calibration rings were measured with strain gages mounted on the outer surfaces and recorded on a digital processing oscilloscope (Norland 2001A Waveform and Data Analysis System). It has sampling rates as fast as one point/μs. It is equipped with a mini-computer and a floppy disk for storage and

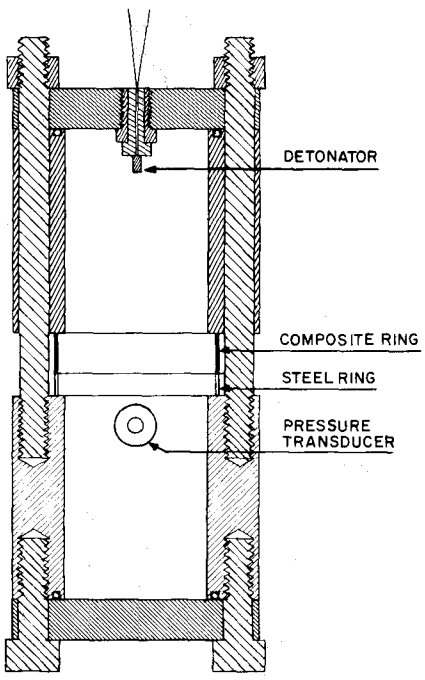

Fig. 1—Fixture for dynamic loading of composite-ring specimens

Fig. 2—Photograph of assembled fixture for dynamic loading of composite ring specimens

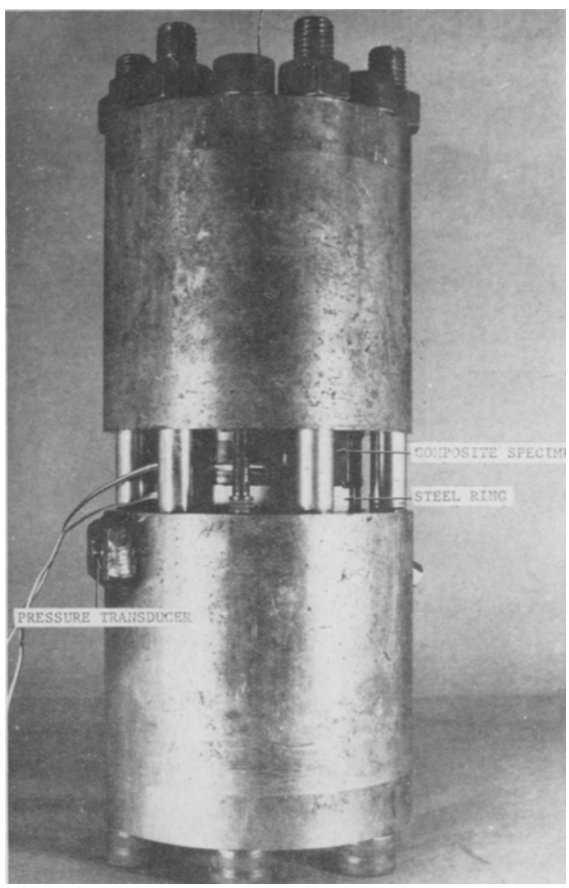

retrieval of data and keystoke programs. It is connected to an X-Y point plotter. Any signal recorded or processed by the oscilloscope or stored in the floppy disk can be plotted to any desired scale.

Data Processing

Data analysis and interpretation are based on the mechanics of a dynamically pressurized elastic ring. The equation of motion for axisymmetric loading is:

$$\frac{\partial \sigma_r}{\partial r} + \frac{\sigma_r - \sigma_\theta}{r} = \varrho \ddot{u} \tag{1}$$

where σ_r, σ_θ the radial and circumferential stresses, r the radial distance, ϱ the material mass density and u the radial displacement. Using the Lamé equations for an internally pressurized cylinder:

$$\sigma_r = \frac{pa^2}{b^2 - a^2}\left(1 - \frac{b^2}{r^2}\right)$$
$$\sigma_\theta = \frac{pa^2}{b^2 - a^2}\left(1 + \frac{b^2}{r^2}\right) \tag{2}$$

the equation of motion at $r = b$ is written as

$$p\left(\frac{2a^2}{b^2 - a^2}\right) = \sigma_\theta + \varrho b \ddot{u} = \sigma_\theta + \varrho b^2 \ddot{\epsilon}_\theta \tag{3}$$

where a and b are the inner and outer radii of the ring.

The primary data recorded in the dynamic ring tests are:

ϵ_θ^s—circumferential strain in steel ring (pressure cell) at the outer radius, b.

ϵ_θ^c—circumferential strain in composite ring at the outer radius, b.

ϵ_x^c—axial strain in composite ring at the outer radius, b.

Assuming a uniaxial state of stress in the circumferential direction, the stress in the elastic ring is computed as

$$\sigma_\theta^s = E^s \epsilon_\theta^s \tag{4}$$

and then, the dynamic pressure is obtained in terms of this stress and the second derivative of ϵ_θ^s

$$p = [\sigma_\theta^s + \varrho_s b_s^2 \ddot{\epsilon}_\theta^s]\left(\frac{b_s^2 - a_s^2}{2a_s^2}\right) \tag{5}$$

where E^s and ϱ_s the modulus and density of steel.

The circumferential stress in the composite ring is obtained in terms of the pressure above and the second derivative of ϵ_θ^c

$$\sigma_\theta^c = p\left(\frac{2a_c^2}{b_c^2 - a_c^2}\right) - \varrho_c b_c^2 \ddot{\epsilon}_\theta^c \tag{6}$$

The dynamic stress-strain curve for the composite material is obtained by plotting σ_θ^c vs. ϵ_θ^c. Moduli, Poisson's ratios, strength and ultimate strain for the composite material are thus obtained from the recorded and computed data.

In the case of the 10-deg off-axis rings used for determination of in-plane shear properties, three-gage rosettes were mounted on the outer surface of the composite rings. The measurements made were:

ϵ_θ^s—circumferential strain in steel ring

ϵ_θ^c—circumferential strain in composite ring

ϵ_x^c—axial strain in composite ring

ϵ_{45}^c—45-deg strain in composite ring

The circumferential stress in the composite ring was obtained from eq (6) as before. The in-plane shear stress, referred to the fiber direction, is given by

$$\sigma_{12}^c = \sigma_\theta^c \sin\phi \cos\phi \tag{7}$$

where $\phi = 10$ deg, the fiber orientation with respect to the circumferential direction. The in-plane shear strain is obtained from the three strain components as follows:

$$\epsilon_{12}^c = \frac{\epsilon_\theta^c - \epsilon_x^c}{2} \sin 2\phi + \left[\epsilon_{45}^c - \frac{\epsilon_x^c + \epsilon_\theta^c}{2}\right] \cos 2\phi \tag{8}$$

A dynamic shear-stress vs. shear-strain curve is obtained by plotting σ_{12}^c vs. ϵ_{12}^c. The shear modulus is given by

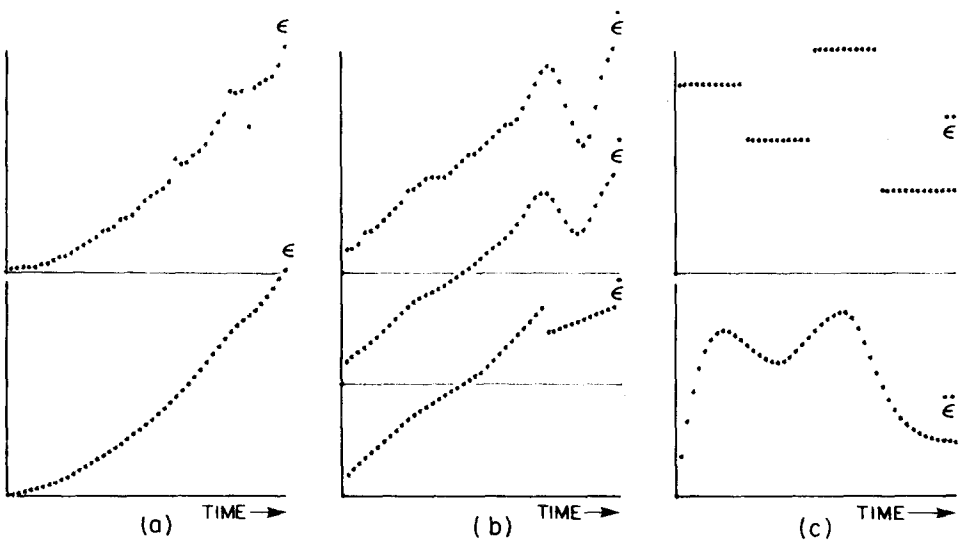

Fig. 3—Illustration of smoothing and approximation operations.
(a) As recorded and smoothed strains;
(b) strain rate, smoothed strain rate and piecewise linear approximation;
(c) stepwise and smoothed strain acceleration

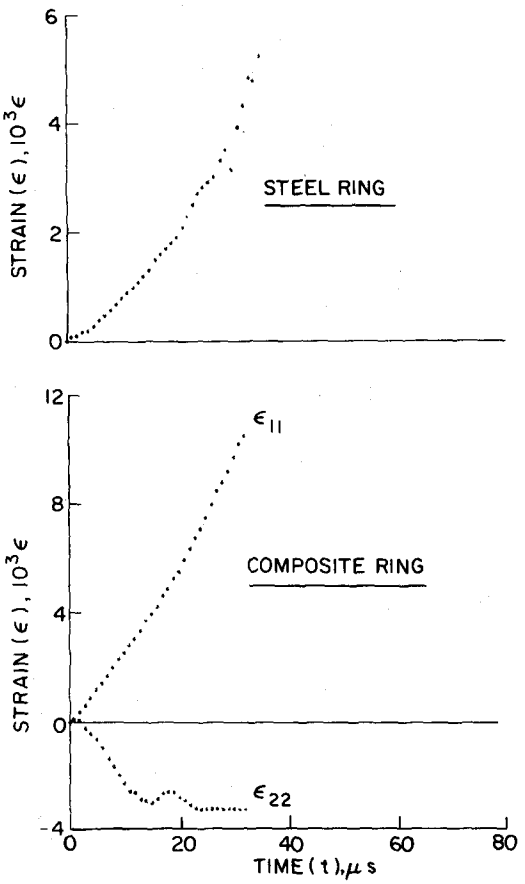

Fig. 4—Strain records in steel ring and [0₆] SP288/AS graphite/epoxy ring under dynamic loading

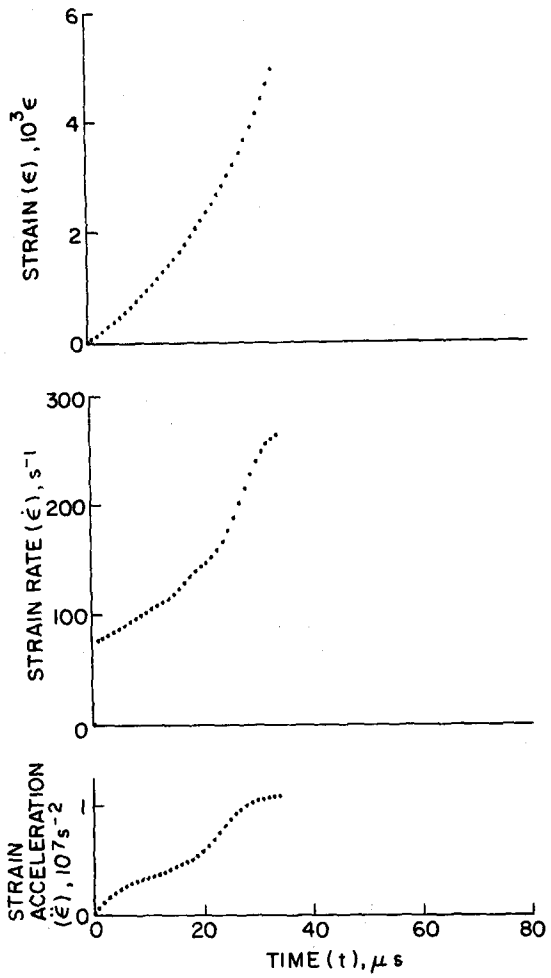

Fig. 5—Strain and its derivatives in steel ring for [0₆] SP288/AS graphite/epoxy test

$$G_{12} = \frac{\sigma_{12}}{2\epsilon_{12}} \tag{9}$$

which can be taken from the initial slope or the secant of the curve.

In the computation above, it is necessary to obtain second derivatives of experimental data, a task which is very difficult to do with precision. The procedure adopted here involves smoothing operations and approximations. The original strain data are smoothed by a three-point averaging technique. Each point on the record, except the first and last ones, is replaced by the average of that point and its two neighboring points. Subsequently, the smoothed curve is differentiated directly on the processing oscilloscope and the derivative curve (strain rate) is smoothed. The smoothed strain-rate curve is then divided into four equal segments and a straight line is fitted in each segment by the least-squares method. Thus, a four-step approximation is obtained of the second derivative (strain acceleration). This four-segment approximation procedure was chosen, as it gave results in agreement with those obtained by graphical (manual) smoothing and differentiation based on experienced judgment and discretion. The discontinuous stepwise curve for the strain acceleration is smoothed by applying the three-point averaging technique seven consecutive times. In this case, an initial point fixed at zero was added to insure that the acceleration correction on the pressure and stress is zero at zero time and strain. The sequence of all these operations is illustrated in Fig. 3 for the circumferential strain in the steel ring, from the as-recorded strain to the smoothed second derivative.

The circumferential strain in the composite ring is treated in an identical manner to arrive at the first and second derivatives.

All smoothing and computational operations were programmed and done automatically in every case. The computer program was stored in the floppy-disk memory of the processing oscilloscope.

Results

Strain and strain-derivative records for a [0₆] graphite/epoxy ring and the steel calibration ring are shown in Figs. 4, 5 and 6. The dynamic stress-strain curve obtained as described before is shown in Fig. 7. Results for four [0₆] composite rings are tabulated in Table 1. The initial strain rate ranges between 170 s^{-1} and 450 s^{-1} and the average (secant) strain rate between 240 s^{-1} and 328 s^{-1}. The initial strain rate is defined as the average slope of the circumferential strain in the composite over the first 10 μs. The secant strain rate is simply the final (ultimate) strain divided by the time to failure. The time to failure

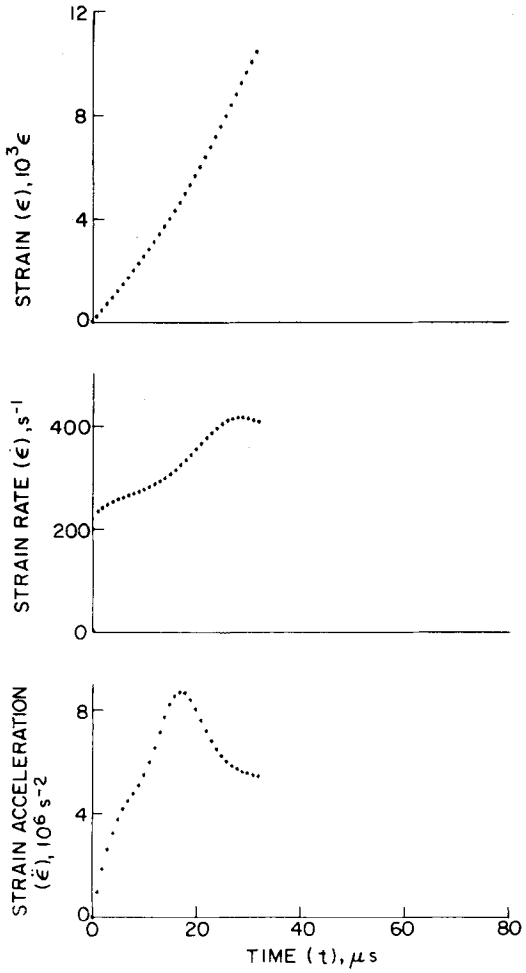

Fig. 6—Circumferential strain and its derivatives for [0_6] SP288/AS graphite/epoxy ring under dynamic loading

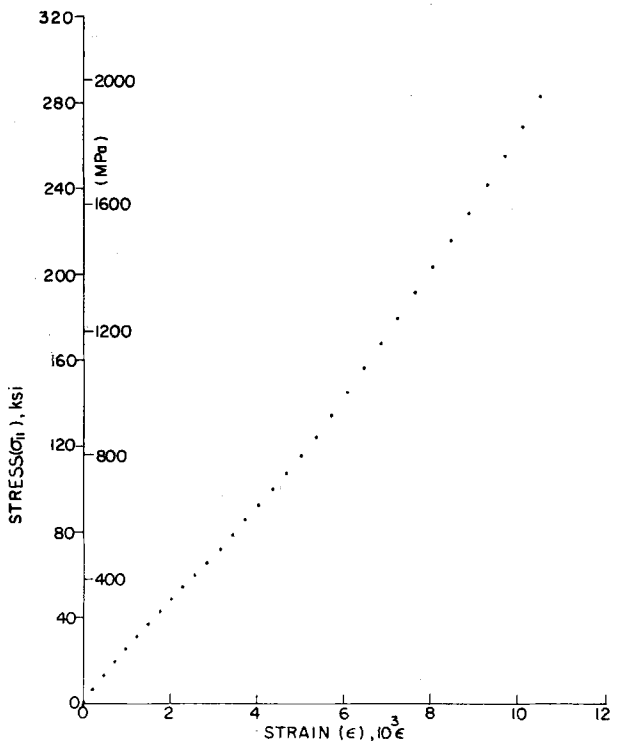

Fig. 7—Stress-strain curve for dynamically loaded [0_6] SP288/AS graphite/epoxy ring

ranges between 31 μs and 37 μs. The average initial and secant moduli are 162.0 GPa (23.48 × 10^6 psi) and 166.8 GPa (24.10 × 10^6 psi), respectively, and exceed the static value of 137 GPa (19.9 × 10^6 psi) by approximately 20 percent. The dynamic Poisson's ratio in this case seems to be appreciably higher than the static value of 0.32. This difference may not be real and may be due to some extraneous axial strain introduced during the dynamic loading. Dynamic strength values show considerable scatter, possibly related to the presence of a seam in the ring specimens. The average dynamic strength of 1511 MPa (219 ksi) is very close to the static strength of 1518 MPa (220 ksi). The average dynamic ultimate strain of 0.0101 is also close to the corresponding static value of 0.0108.

Strain records for a [90_8] composite ring and the steel calibration ring are shown in Fig. 8. The data were processed as discussed before and a dynamic stress-strain curve was obtained and plotted (Fig. 9). Results for three [90_8] composite rings are tabulated in Table 2. The initial strain rate varies between 25 s^{-1} and 120 s^{-1} and the average (secant) rate between 128 s^{-1} and 195 s^{-1}. The time to failure ranges between 40 μs and 50 μs. The average initial and secant moduli of 41.3 GPa (5.99 × 10^6 psi) and 21.0 GPa (3.04 × 10^6 psi), respectively, are much higher than the static modulus of 10.4 GPa (1.51 × 10^6 psi). The dynamic Poisson's ratio is a little higher (in

TABLE 1—HIGH-STRAIN-RATE TENSILE PROPERTIES OF [0_6] SP288/AS GRAPHITE EPOXY

Specimen No.	Strain Rate ($\dot{\epsilon}_{11}$), s^{-1}	Modulus (E_{11}), GPa (10^6 psi)	Poisson's Ratio (ν_{12})
	Initial Properties		
7-6	170	155.9 (22.60)	—
7-7	250	176.6 (25.60)	0.55
7-8	260	163.7 (23.72)	0.41
7-9	450	151.8 (22.00)	0.40
	Secant Properties		
7-6	240	134.9 (19.56)	—
7-7	328	203.5 (29.49)	0.32
7-8	316	163.3 (23.67)	0.54
7-9	314	165.6 (24.00)	0.55
	Ultimate Properties		
	Time to Failure (t_f), μs	Strength (S_{11T}), MPa (ksi)	Strain (ϵ_{11T}^u)
7-6	37	1214 (176)	0.0090
7-7	32	2136 (310)	0.0105
7-8	31	1601 (232)	0.0098
7-9	35	1090 (158)	0.0110

absolute terms) than the static value of 0.03. The average dynamic strength of 146.3 MPa (21.2 ksi) is much higher than the static strength of 64 MPa (9.3 ksi). The average dynamic ultimate strain of 0.0069 is very close to the corresponding static value of 0.0066.

Strain records for a $[10_8]$ composite ring and the steel calibration ring are shown in Fig. 10. These data were processed as discussed before and a dynamic shear-stress vs. shear-strain curve was obtained and plotted (Fig. 11). Results for three $[10_8]$ composite rings are tabulated in Table 3. Initial strain rates vary between 140 s^{-1} and 170 s^{-1} and average (secant) rates vary between 223 s^{-1} and 282 s^{-1}. The time to failure ranges between 40 μs and 47 μs. The average initial shear modulus of 8.26 GPa (1.20×10^6 psi) is also higher than the static modulus of 6.3 MPa (0.91×10^6 psi). The average dynamic shear strength of 113 MPa (16.4 ksi) is also noticeably higher than the static strength of 87 MPa (12.6 ksi). The average dynamic ultimate shear strain of 0.0108 is lower than the static value of 0.0137.

Summary and Conclusions

A method is described for testing composite materials at strain rates in the 100 s^{-1} to 500 s^{-1} regime. The method utilizes a thin ring specimen loaded by an internal pressure pulse applied explosively through a liquid. Strains in the composite specimen and in a steel calibration ring were recorded with a digital processing oscilloscope.

Data analysis was based on a numerical solution of the equation of motion. A computer program was written involving smoothing and approximations of the strain data, strain rate and strain acceleration. Dynamic stress-strain curves were obtained and plotted for 0-deg, 90-deg and 10-deg off-axis graphite/epoxy specimens.

In the case of 0-deg specimens, the dynamic modulus exceeds the static by approximately 20 percent, whereas, the dynamic strength and dynamic ultimate strain are very close to the corresponding static values. In the transverse to the fiber direction, the dynamic modulus and strength are two to four times the corresponding static values, whereas the dynamic ultimate strain is close to the static one. The in-plane dynamic shear modulus and shear strength are approximately 30 percent higher than the static values. However, the dynamic ultimate shear strain

TABLE 2—HIGH-STRAIN-RATE TENSILE PROPERTIES OF $[90_8]$ SP288/AS GRAPHITE/EPOXY

Specimen No.	Strain Rate ($\dot{\epsilon}_{22}$), s^{-1}	Modulus (E_{22}), GPa (10^6 psi)	Poisson's Ratio (ν_{21})
		Initial Properties	
5-9	25	28.6 (4.15)	0.06
5-10	120	42.8 (6.20)	—
5-11	70	52.6 (7.62)	—
		Secant Properties	
5-9	128	24.8 (3.59)	0.05
5-10	195	18.9 (2.74)	—
5-11	136	19.2 (2.78)	—
		Ultimate Properties	
	Time to Failure (t_f), μs	Strength (S_{22T}), MPa (ksi)	Strain (ϵ^u_{22T})
5-9	50	159 (23.0)	0.0064
5-10	40	157 (22.8)	0.0078
5-11	47	122 (17.8)	0.0064

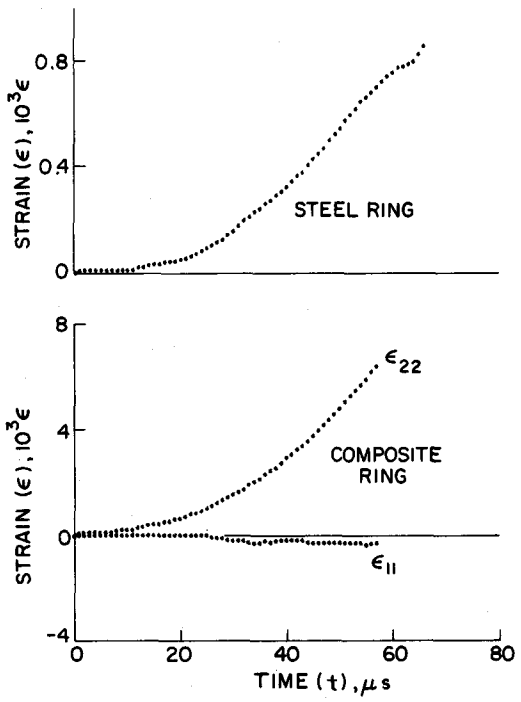

Fig. 8—Strain records in steel ring and $[90_8]$ SP288/AS graphite/epoxy ring under dynamic loading

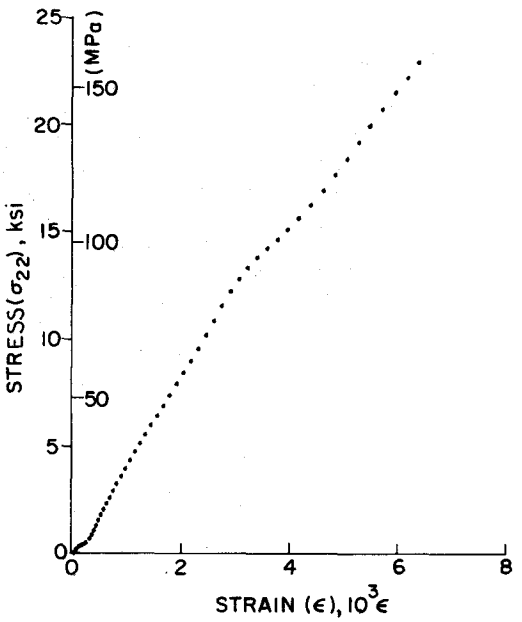

Fig. 9—Stress-strain curve for dynamically loaded $[90_8]$ SP288/AS graphite/epoxy ring

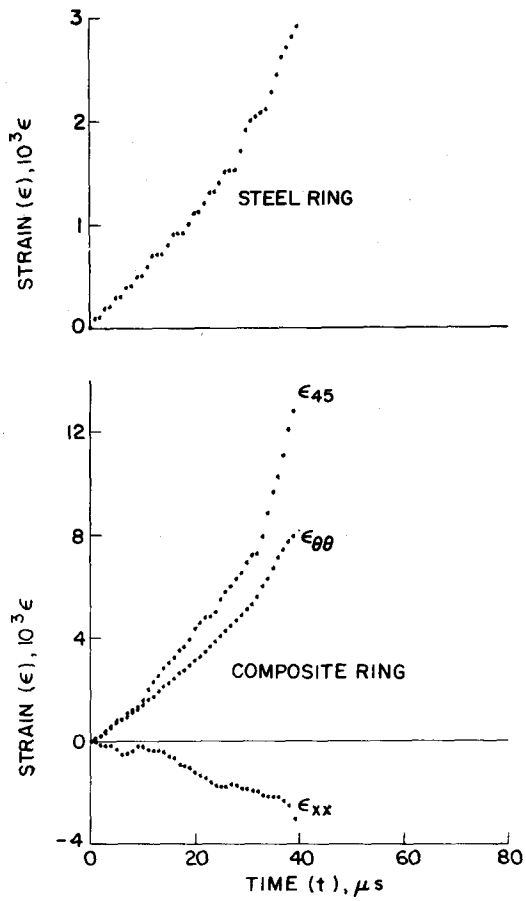

Fig. 10—Strain records in steel ring and in [10_8] SP288/AS graphite/epoxy ring under dynamic loading

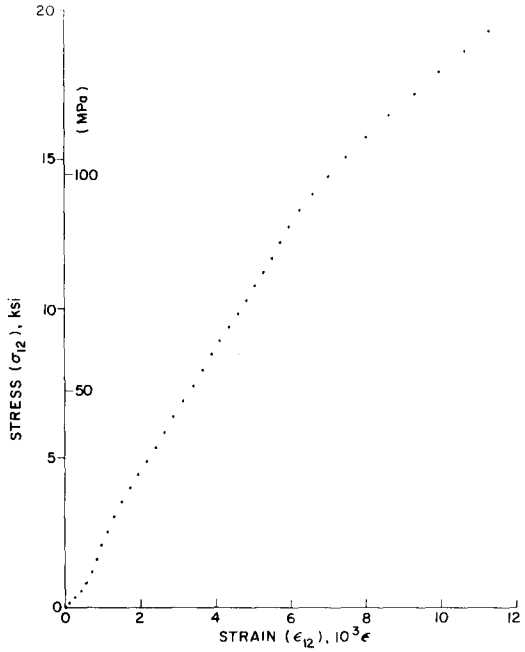

Fig. 11—Shear-stress vs. shear-strain curve for dynamically loaded [10_8] SP288/AS graphite/epoxy ring

is lower than the static one, because the nonlinearity of the shear stress-strain curve is less pronounced under dynamic conditions.

Acknowledgment

The work described here was sponsored by the NASA-Lewis Research Center, Cleveland, OH. We are grateful to C.C. Chamis of NASA-Lewis for his encouragement and cooperation.

References

1. *Zimmer, J.E. and Cost, J.R., "Determination of the Elastic Constants of a Unidirectional Fiber Composite Using Ultrasonic Velocity Measurements," J. Acoust. Soc. of Amer.,* **47** *(3), 795-803 (1970).*

2. *Gieske, J.H. and Allred, R.E., "Elastic Constants of B-Al Composites by Ultrasonic Velocity Measurements,"* EXPERIMENTAL MECHANICS, **14** *(4), 158-165 (April 1974).*

3. *Gibson, R.F. and Plunkett, R., "Dynamic Mechanical Behavior of Fiber-Reinforced Composites: Measurements and Analysis," J. Comp. Mat'ls.,* **10**, *325-341 (Oct. 1976).*

4. *Rotem, A. and Lifshitz, J., "Longitudinal Strength of Unidirectional Fibrous Composite Under High Rate of Loading," Proc. of 26th Ann. Tech. Conf., 1972, Reinforced Plastics/Composites Div., The Soc. of Plastics Ind., Sec. 10-G (Feb. 1971).*

5. *Lifshitz, J., "Impact Strength of Angle Ply Fiber Reinforced Materials," J. Comp. Mat'ls.,* **10**, *92-101 (Jan. 1976).*

6. *Armenakas, A.E. and Sciammarella, C.A., "Response of Glass-fiber-reinforced Epoxy Specimens to High Rates of Tensile Loading,"* EXPERIMENTAL MECHANICS, **13** *(10), 433-440 (Oct. 1973).*

7. *Daniel, I.M. and Liber, T., "Strain Rate Effects on Mechanical Properties of Fiber Composites," IITRI Report D6073-IV, for NASA-Lewis Research Center, NASA CR-135087 (June 1976).*

8. *Daniel, I.M. and Liber, T., "Testing of Fiber Composites at High Strain Rates," Proc. 2nd Int'l Conf. on Comp. Matls. ICCM/2, Toronto, Canada, 1003-1018 (April 1978).*

9. *Sierakowski, R.L., Nevill, G.E., Ross, C.A. and Jones, E.R., "Dynamic Compressive Strength and Failure of Steel Reinforced Epoxy Composites," J. Comp. Mat'ls.,* **5**, *362-377 (July 1971).*

10. *Liber, T., Daniel, I.M., LaBedz, R. and Niiro, T., "Fabrication and Testing of Composite Ring Specimens," 34th Annual Technical Conference, 1979, Reinforced Plastics/Composites Institute, The Society of the Plastics Industry, Inc., Sect. 22-B (Feb. 1979).*

TABLE 3—IN-PLANE SHEAR PROPERTIES OF UNIDIRECTIONAL GRAPHITE/EPOXY

Specimen No.	Strain Rate ($\dot{\epsilon}_{12}$), s^{-1}	Shear Modulus (G_{12}), GPa (10^6 psi)
	Initial Properties	
15-5	170	7.08 (1.03)
15-7	140	10.09 (1.46)
15-8	160	7.80 (1.13)
	Secant Properties	
15-5	223	5.34 (0.77)
15-7	230	4.77 (0.69)
15-8	282	5.56 (0.81)

	Ultimate Properties		
	Time to Failure (t_f), μs	Strength (S_{12}), MPa (ksi)	Strain (ϵ_{12}^u)
15-5	47	112 (16.3)	0.0105
15-7	46	100 (14.6)	0.0106
15-8	40	126 (18.2)	0.0113